Electrical Conduc+E23:P24tivity of the Coexisting System Containing Molten Carbonates and Rare-earth Oxide

Mizuhata, Minoru
Ohashi, Toshifumi
Béléké, Alexis Bienvenu

(Citation)
ECS Transactions,33(7):439-447

(Issue Date)
2010

(Resource Type)
journal article

(Version)
Version of Record

(URL)
https://hdl.handle.net/20.500.14094/90005896

ECS Transactions, 33 (7) 439-447 (2010)
10.1149/1.3484802 ©The Electrochemical Society

Electrical Conductivity of the Coexisting System Containing Molten Carbonates and Rare-earth Oxide

Minoru Mizuhata, Toshifumi Ohashi, and Alexis Bienvenu Béléké

Department of Chemical Engineering, Graduate School of Engineering, Kobe University
1-1 Rokkodai-cho, Nada, Kobe, 657-8501 Japan

The electrical, thermal and structural properties of $CeO_2/(Li_{0.52}Na_{0.48})_2CO_3$ coexisting system are investigated by AC impedance, differential thermal analysis and polarized Raman scattering spectroscopy. The system shows a dependence of the electrical conductivity upon the temperature. The transition point varies with the apparent average thickness of the liquid phase, while the activation energy, ΔE_a, remains constant at any distance from the solid phase. The symmetric stretching mode of the polarized Raman spectra shows that carbonate ion maintains its D_{3h} symmetry in the presence of ceria. A constant value of the depolarization ratio of the $\nu_1(A'_1)$ mode with regard to the apparent average thickness confirms that the symmetry of carbonate ions in the molten state is not altered by the presence of ceria powder. These findings contribute to the understanding of the properties of ceria-based carbonate electrolyte for intermediate temperature fuel cells.

Introduction

Molten salts permeated among highly dispersed inorganic particles are applied in various fields such as the synthesis of inorganic materials, batteries, fuel cells, crystal growth, or liquid-phase sintering process of ceramics. We have demonstrated in the past that the coexistence of molten salt electrolytes with inorganic materials, in some cases, leads to interactions between the two phases. Such interactions play a crucial role in the physical and chemical properties of the conductive ionic species (1-6). For example in the conventional MCFCs, insulating oxides such as γ-$LiAlO_2$ powder are utilized as the matrix of molten carbonate tile. In such a system, the melting or eutectic points of carbonate decreases with an increase of the surface area of solid phase and the activation energy increases with the average thickness of the melt on the solid surface (2-3,5-6). Therefore, a better understanding of the behavior of ionic species at the vicinity of the solid materials is appealing from the viewpoint of the development of advanced technologies.

Molten carbonate electrolytes find tangible applications in stationary power generation fuel cell systems such as molten carbonate fuel cells (MCFCs) (7, 8), intermediate temperature solid oxide fuel cell (IT-SOFCs) (8, 9) and, direct carbon fuel cells (DCFCs) (10) All these molten-salts fuel cells operate at higher temperature, and still present major technical issues as well as economic challenges delaying their commercialization (11). There is a great demand for alternative fuel cells operating at

moderate temperatures. In this context, intermediate temperature (400 ~ 800^{o}C) fuel cells are very attractive since they combine the advantages of both high and low temperature fuel cells such as fast electrode kinetics, fuel flexibility and less degradation problems (12). Furthermore, the tendency of lower temperatures makes the conventional ceramic fuel cells (mainly solid oxide fuel cells (SOFCs)) a leading candidate for application as stationary power plants but also the possibility to replace internal combustion engines in vehicles (13). Ceramic fuel cells based on ceria-carbonate salt composite electrolytes have been intensively studied for the past decade due to their reliable ionic lattice conductivity and stability at intermediate temperature (14, 15). Although major challenges such as fabrication of thin electrolyte by conventional method and development of high-performance cathode materials have been addressed, less attention has been devoted to the interactions between molten salts and porous solid materials. In this study, the physical and chemical properties of CeO_2/molten $(Li/Na)_2CO_3$ composite are investigated. The ionic conductivity and the temperature dependence at the solid/melt interface are discussed. The activation energy of the electrical conductivity and the thermal behavior of the anionic species are compared with the systems containing alumina powders. The aim is to clarify the properties of molten carbonate electrolyte coexisting with ceria powder in intermediate temperature fuel cells.

Experimental

High purity CeO_2 powder (Nacalai Tesque, Inc.) with specific surface areas 1.5 and 6.0 m^2/g were employed as the solid phase while a mixture of Li_2CO_3 and Na_2CO_3 (Nacalai Tesque, Inc.) in a ratio of 52:48 wt% was used as the liquid phase. The solid phase and each of the carbonate salts were annealed at 873 K for 2 h and 473 K for 48h in N_2 gas flow, respectively prior to measurements. The dehydrated eutectic $(Li_{0.52}Na_{0.48})_2CO_3$ was prepared by mixing guaranteed reagents Li_2CO_3 and Na_2CO_3 at 873K in CO_2 gas flow. A Li/Na binary carbonate and oxide powder were mixed in alumina agate mortar and molded into a tablet sample. The liquid content varied from 5 – 45 vol.%.

AC impedance was measured under CO_2, N_2 and Air atmosphere with LCR precision meter HP 4284A using a platinum (Pt) electrode in a frequency range 20Hz ~ 1MHz and the output voltage of 0.6 V. The temperature range was 673 ~ 823K. The electrical conductivity was calculated from the Nyquist plots.

Raman spectra were recorded with a HORIBA Ramanor T-64000 spectrometer equipped with an optical alignment for polarized Raman, monochromator with AABSPEC #2000-A. The excitation source was a 532 nm SHG of Nd:YVO_4 laser with a power of 20 mW at the sample point. Differential thermal analysis (DTA) measurements were carried out with Rigaku Thermo Plus under CO_2 gas during all the measurements. 10 mg of ceria oxides/carbonate salts was loaded into an Au pan (ϕ = 5 mm). The temperature range was 573-873 K and the scanning rate was 10 K/min in all cases.

Results and discussion

Temperature dependence of the electrical conductivity

Figure 1 shows typical temperature dependence of the electrical conductivity for the systems CeO_2 (1.5m^2/g) / $(Li_{0.52}Na_{0.48})_2CO_3$ (a) and CeO_2 (6.0 m^2/g)/ $(Li_{0.52}Na_{0.48})_2CO_3$ (b) with various melt contents. In both cases, the electrical conductivity increases with increasing temperature up to the melting point of each composition, wherein an abrupt change appears. Then the linearity of the Arrhenius plot (log σ versus *1/T*) is observed. The curves show that the electrical conductivity still possesses a significant value below the melting point. Furthermore, the electrical conductivity increases with increasing carbonate volume fraction. A similar tendency was observed by Zhu et al. (16) for SDC-carbonate electrolyte above 500 ^oC. The corresponding variation of the transition point, T_t, as a function of the apparent average thickness of the liquid phase is plotted and compared with that of α-Al_2O_3 in Figure 2. It is obvious that the transition point for ceria samples is lower than that of alumina, which is related to intrinsic properties of each material. In both cases, the transition point showed a similar behavior: it slowly decreases with decreasing apparent average thickness up to ca. 12 nm wherein a drastic decrease is observed. It is suggested that the transition point depends on the composition of the solid/liquid coexisting system. In our previous work related to γ-$LiAlO_2$ and MgO powder coexisting with Li_2CO_3, we have shown that the lowering of the transition point was caused by the interactions between the solid and liquid phase. We suggested that carbonates interact with the solid phase, and a small amount of stable unfrozen liquid exist on the solid phase which contributes to the conduction (2-3, 5). A similar phenomenon was observed by Liang in the study of binary solid electrolyte-metal oxide particles of which the author called "conductivity enhancement effects" (17). These results indicate that near the solid surface, the conductivity and phase transition of carbonates are strongly influenced by the presence of the solid phase.

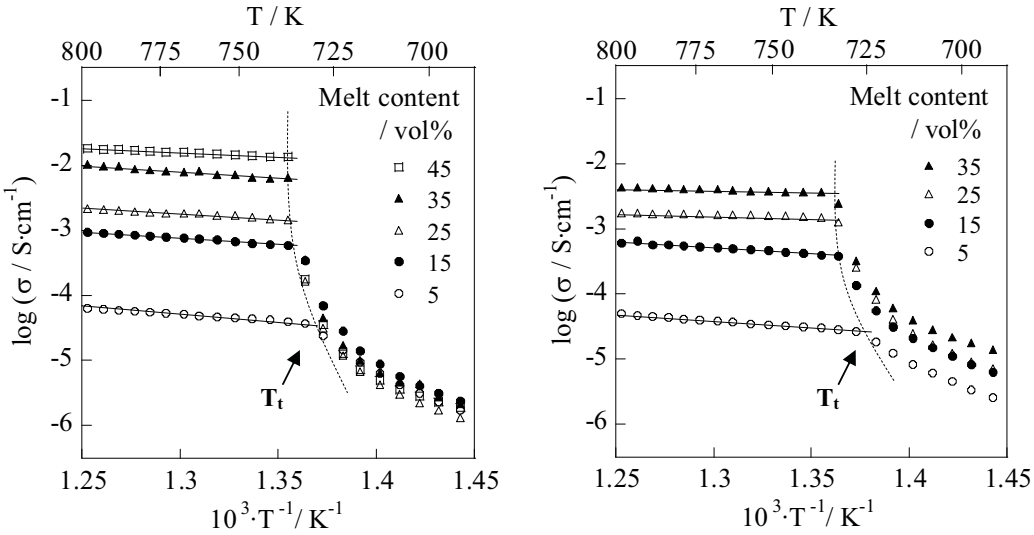

Figure 1. Temperature dependence of the electrical conductivity for the system: (a) CeO_2(1.5 m^2/g)/$(Li_{0.52}Na_{0.48})_2CO_3$ and, (b) CeO_2(6.0 m^2/g)/$(Li_{0.52}Na_{0.48})_2CO_3$

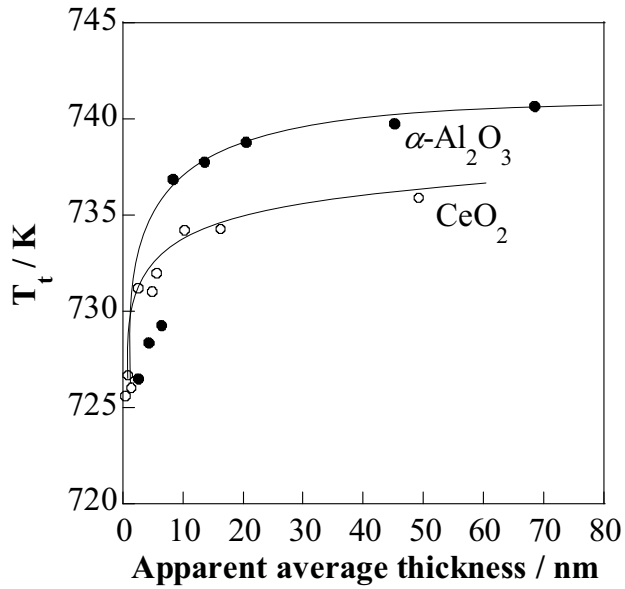

Figure 2. Variation of the transition point as a function of the apparent average thickness of the liquid layer for $CeO_2/(Li_{0.52}Na_{0.48})_2CO_3$ and α-Al_2O_3 /$(Li_{0.52}Na_{0.48})_2CO_3$ systems.

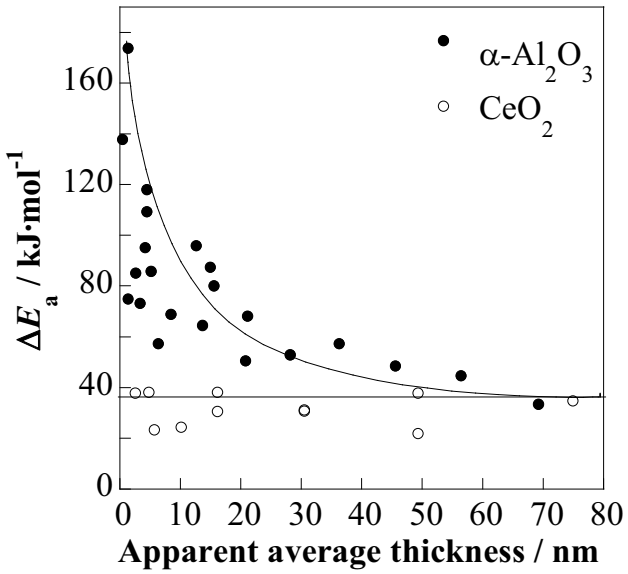

Figure 3. Variation of the activation energy as a function of the apparent average thickness of the liquid layer for $CeO_2/(Li_{0.52}Na_{0.48})_2CO_3$ and α-Al_2O_3 /($Li_{0.52}Na_{0.48})_2CO_3$ systems.

The variation of the activation energy with the apparent average thickness of the liquid layer for the system CeO_2 ($1.5m^2/g$)/ $(Li_{0.52}Na_{0.48})_2CO_3$ is shown in Figure 3. For comparison purpose, data for the system containing α-Al_2O_3/ $(Li_{0.52}Na_{0.48})_2$ CO_3 are also displayed. The electrical conductivity was determined according to Arrhenius equation shown below:

$$\log \sigma = -\Delta E_a/2.303RT + \log a \qquad [1]$$

where σ is the electrical conductivity, ΔE_a the activation energy, R the gas constant, a the frequency factor (constant), and T the absolute temperature. It can be easily noticed that the activation energy for CeO_2/molten $Li_xNa_{1-x}CO_3$ remains constant in the whole range of the same liquid content while that of α-Al_2O_3 powder system increases with decreasing apparent average thickness of the liquid phase. This result is quite interesting because it suggests that for ceria system the activation energy is not influenced by the presence of the solid phase, as it has been reported for other inorganic powder coexisting with molten carbonates (2-3, 5-6). It is assumed that the surface conducting behavior is governed by the ionic conductor at the surface of ceria oxide. It is known that three kinds of conductive ionic species; CO_3^{2-}, H^+, and O^{2-} are involved in/on CeO_2. Of these, it has been reported that the transport number of CO_3^{2-} in samarium doped carbonate (SDC) at 550 ^oC is 0.67 which is higher than those of H^+ (0.09) and O^{2-} (0.24). This clearly signifies that the contribution of CO_3^{2-} is predominant (16). Therefore, the activation energy in this case might be indicated as the transport on the solid surface.

Melting behavior

In order to observe the melting behavior of carbonate near the solid phase, the thermal analysis of the heterogeneous systems was performed. Figure 4 shows that DTA curves of the CeO_2 ($1.5m^2/g$)/$(Li_{0.52}Na_{0.48})_2CO_3$ system with various melt contents. For each sample, the endothermic peak showing the melting of carbonate salt is observed. The peaks tops shift toward lower temperature with decrease of carbonate content. The shift of the endothermic peak corresponding to the fusion of carbonates signifies that the molten state of carbonate was stabilized by the presence of inorganic powder below each melting point. This lowering of the melting temperature is attributed to the effects of the solid phase. These features are consistent with the temperature dependence of the electrical conductivity above mentioned. The intensity of the endothermic peak increases with increasing carbonate content (2-3, 5). As mentioned above, we have studied the electrical conductivity of ceria coexisting with carbonate salts and observed a dependence of the electrical conductivity on the temperature. In this section, a comparison between the transition temperature, T_t of the electrical conductivity and the peak-top temperature, T_m of the DTA for the CeO_2 /$(Li_{0.52}Na_{0.48})_2CO_3$ coexisting system is done. T_t can be understood as the point at which ions are able to move perfectly as liquid state in other terms, the *apparent melting point* of the electrical conductivity whereas, T_m can be considered as the point at which salt are completely fused or the *apparent melting point* of DTA. The variation of T_t of the electrical conductivity is plotted versus the peak-top temperature, T_m of the DTA in Figure 5. It can be seen that there is a linear relationship between these two temperature parameters, despite the fact that they stem from different properties. That signifies the existence of a correlation between the transport property defined here by the electrical conductivity and the endothermic phenomenon of salt based on the thermal analysis. It also appears on this figure that T_m is higher than T_t.

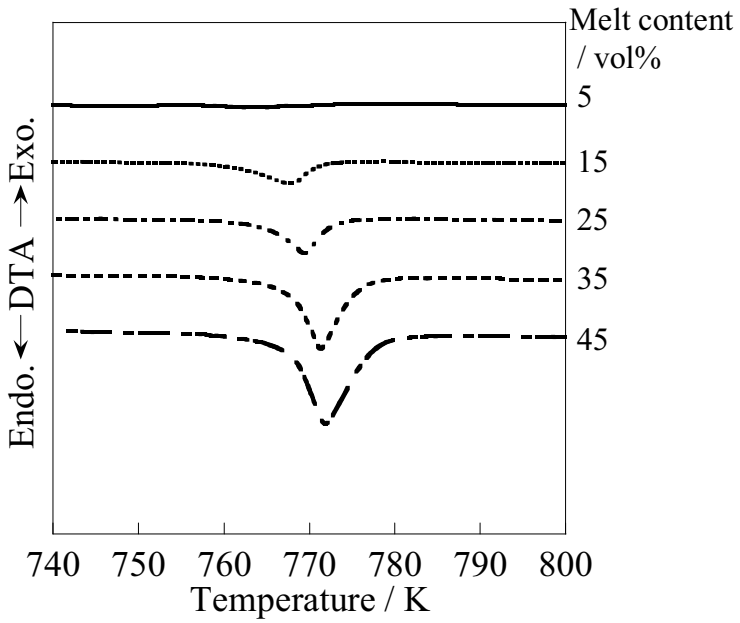

Figure 4. DTA curves for CeO_2(1.5 m^2/g)/$(Li_{0.52}Na_{0.48})_2CO_3$ system at various melt contents.

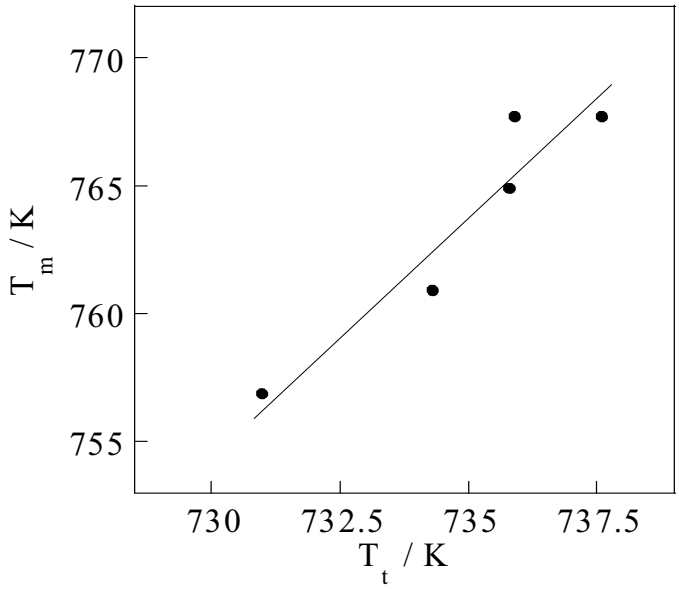

Figure 5. Relationship between the transition temperature of the electrical conductivity T_t, and the melting point of eutectic carbonate, T_m for CeO_2/($Li_{0.52}Na_{0.48})_2CO_3$ coexisting system.

Raman spectra of molten carbonate

In order to investigate the effects of ceria powder on the structure of molten carbonates, polarized Raman spectroscopy measurements were carried out. The planar carbonate ion (CO_3^{2-}) is known to belong to the point group D_{3h} and has four fundamental vibration modes: (*i*) symmetric stretching vibration, $\nu_1(A'_1)$ Raman active only (polarized), (*ii*) out-of-plane bending, $\nu_2(A''_2)$ infrared active only, (*iii*) doubly degenerate asymmetric stretch, $\nu_3(E')$, and (*iv*) another doubly degenerate bending mode, $\nu_4(E')$ Raman (depolarized) and infrared active (18). The exact frequencies depend on the crystal structure and the associated cation. In condensed states such as solid and liquid, environmental effects are frequently sufficient to reduce the local symmetry from D_{3h} to C_{2v} or C_s, which may result in splitting of the degenerate modes, ν_3 and ν_4, and in the case of substantial interaction, by appearance of ν_1 in the infrared spectrum and ν_2 in the Raman spectrum. Polarized Raman spectra showing the symmetric stretching vibration mode, $\nu_1(A'_1)$ of molten eutectic $(Li_{0.52}Na_{0.48})_2CO_3$. and CeO_2 (1.5m^2/g)/$(Li_{0.52}Na_{0.48})_2CO_3$ with 45 vol. % of melt content are displayed in Figure 6. $\nu_1(A'_1)$ appears at 1061 cm^{-1} in the bulk (Figure 6a) and slightly shifts to 1064 cm^{-1} in ceria system (Figure 6b). This slight shift indicates that free D_{3h} carbonate anions are not significantly perturbed by the presence of ceria powder.

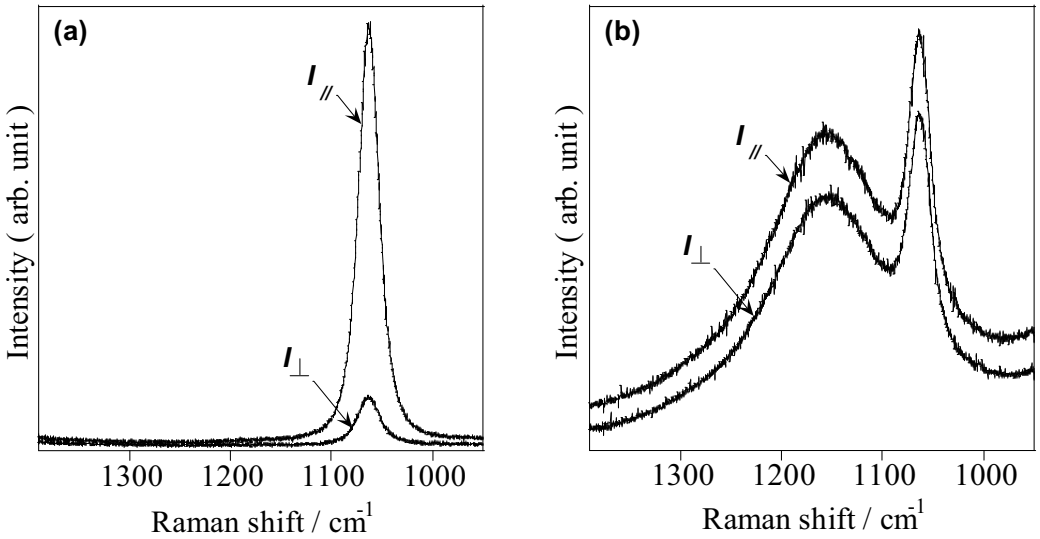

Figure 6. Polarized Raman spectra showing the $\nu_1(A')$ stretching mode of CO_3^{2-} ions in the system: (a) $(Li_{0.52}Na_{0.48})_2CO_3$ and (b) CeO_2 /($Li_{0.52}Na_{0.48})_2CO_3$.

The variation of the depolarization ratios of the $\nu_1(A'_1)$ mode as a function of the apparent average thickness for the systems ceria/carbonate and alumina/carbonate are shown in Figure 7. Raman depolarization ratio is a powerful tool to provide useful information on molecular symmetry in liquids and solutions. The depolarization ratio calculated for bulk $(Li_{0.52}Na_{0.48})_2CO_3$ is ca. 0.30, which indicates that the symmetry of CO_3^{2-} ion is slightly distorted by the presence of alkali cation. Although the

depolarization ratios for all the coexisting systems appear above the theoretical value of 0.75, the depolarization ratio for ceria system did not show any significant change with the apparent average thickness, whereas that for alumina samples exponentially increases with the decrease of the apparent average thickness of the liquid layer. This result confirms that the chemical structure of carbonate ion is not significantly influenced by the ceria oxide as solid phase. The breakdown of the polarization rule according to the "Placzek Polarizability Theory" (19) could be interpreted as anomalous polarization (20-22).

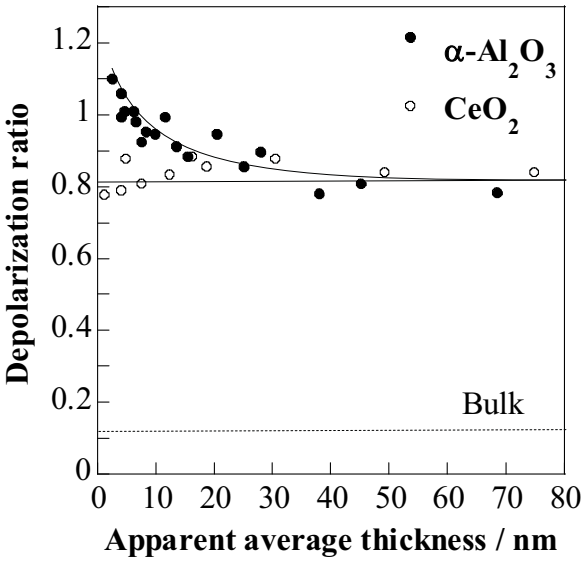

Figure 7. Variation of the depolarization ratio of the Raman $\nu_1(A')$ stretching mode of CO_3^{2-} ions as a function of the apparent average thickness for $CeO_2/(Li/Na)_2CO_3$ and α-$Al_2O_3/(Li/Na)_2CO_3$.

Conclusion

The physical and chemical properties of CeO_2 /$(Li_{0.52}Na_{0.48})_2CO_3$ coexisting system have been studied. The electrical conductivity increased with increasing temperature up to the melting point before the appearance of the linear Arrhenius plot. It is assumed that the electrical conductivity still possess a significant value below the melting point. The variation of the transition point as a function of apparent average thickness of the liquid phase indicates that both ceria and alumina composites display a similar thermal behavior; the transition point of carbonate salts was lowered by the existence of the solid phase. However, difference in the variation of the activation energy with the apparent average thickness of the liquid phase for the two systems shows that ceria-carbonate

electrolytes exhibit higher electrical properties than alumina-carbonate electrolytes. A correlation was found between the transition point, T_t, of electrical conductivity and the melting point, T_m of ceria systems. Polarized Raman spectra show that the symmetric stretching mode of carbonate is slightly perturbed by the solid phase. This assertion is confirmed by the depolarization ratio which remains constant at any range of the apparent average thickness. Finally, it can be concluded that carbonate melts in coexisting system show a similar thermal behavior with ceria and alumina powders, but different electrical and structural properties.

References

1. A. B. Béléké, M. Mizuhata, A. Kajinami, and S. Deki, *J. Colloid Interface Sci.*, **268**, 413 (2003).
2. M. Mizuhata, Y. Harada, G. Cha, A. B. Béléké, and S. Deki, *J. Electrochem. Soc.*, **151**, E179 (2004).
3. M. Mizuhata and S. Deki, *J. Rare Earths,* **23,** 1(2005).
4. A. B. Béléké, M. Mizuhata, and S. Deki, *Vibrational Spectrosc.,* **40**, 66(2006).
5. M. Mizuhata, A. B. Béléké, H. Watanabe, Y. Harada, and S. Deki, *Electrochem. Acta.*, **53**, 71(2007)
6. M. Mizuhata, T. Ohta, and S. Deki, *Electrochemistry,* **77**, 721(2009)
7. M. Cassir and C. Belhomme, *Plasmas & Ions,* **1**, 3(1999)
8. C. Xia, Y. Li, Y. Tian, Q. Liu, Y. Zhao, L. Jia, and Y. Li, *J. Power Sources,* **188,** 156 (2009).
9. Q. X. Fu, S. W. Zha, W. Zhang, D. K. Peng, G. Y. Meng, and B. Zhu, *J. Power Sources,* **104**, 73(2002).
10. L. Jia, Y. Tian, Q. Liu, C. Xia, J. Yu, Z. Wang, Y Zhao, and Y. Li,, *J. Power Sources,* **195**, 5581(2010)
11. J. R. Selman, *J. Power Sources,* **160,** 852(2006).
12. S. Zha, J. Cheng, Q. Fu, and G. Meng, *Mater Chem. Phys.,* **77,** 594(2002).
13. R. Doshi, V. L. Richards, J. D. Carter, X. Wang, and M. Krumpelt *J. Electrochem. Soc*., **146,** 1273(1999).
14. C. Milliken, S. Guruswamy, and A. Khandkar *J. Electrochem. Soc.,* **146,** 872(1999).
15. B. C. H. Steele, *Solid State Ionics,* **129,** 95(2000).
16. W. Zhu, C. Xia, D. Ding, X. Shi, and G. Meng, *Mater. Res. Bull.,* **41**, 2057(2006).
17. C. C. Liang *J. Electrochem. Soc.,* **120**, 1289(1973).
18. K. Nakamoto, Infrared and Raman Spectra of Inorganic and Coordination Compounds 5th ed. Part A. Theory and Applications in Inorganic Chemistry, Wiley, 550 New York, 1997.
19. G. Z. Placzek, *Physik,* **70,** 84(1934).
20. A. Warshel, *Chem. Phys. Lett.,* **23,** 273(1976).
21. H. Hamaguchi, *J. Chem. Phys.,* **66,** 5757 (1976).
22. Y. Saito, T. Ishibashi, and H. Hamaguchi, *J. Raman Spectrosc.,* **34,** 725 (2000).